Published by :
http://www.ijert.org

International Journal of Engineering Research & Technology (IJERT)
ISSN: 2278-0181
Volume 13, Issue 02, February 2024

Response Surface Methodology Optimization of Mig Welding Process by Taguchi Method on Ferritic Stainless Steel

Sai Kumar Samala
Cyient
Hyderabad, Telangana, India

G Praveen Kumar
Cyient
Hyderabad, Telangana, India

***Abstract*— In the context of metal inert gas (MIG) welding, precise control over welding parameters significantly impacts the quality of welded joints. Extensive testing and analysis are essential to achieve the desired quality attributes in welded specimens. The current study aims to investigate how welding parameters—specifically welding current, gas flow rate, and nozzle-to-plate distance—affect the percentage elongation (PE) and ultimate tensile strength (UTS) of AISI409 ferritic stainless steel during MIG welding. Experiments based on the Taguchi method's L9 orthogonal array have been conducted. Additionally, visual inspections and X-ray radiography tests have revealed defects both on the surface and beneath the welded specimens.**

***Keywords*—component; formatting; style; styling; insert (key words)**

I. INTRODUCTION

Ferritic stainless steel, containing 11–12% chromium, serves as an affordable utility stainless steel. Developed to bridge the gap between rust-prone carbon steel and stainless steel, ferritic steels combine the technical advantages of carbon steel with those of stainless steel. Unlike austenitic steels, ferritic steels exhibit body-centered cubic crystals, possess less ductile properties, and cannot be heat-treated to achieve hardness like martensitic steel. Generally, ferritic stainless steel is considered to have poorer weldability compared to austenitic stainless steel. The older ferritic grades, such as AISI 409 & 430, find widespread use in home appliances and other applications

Nomenclature

C	welding current
G	gas flow rate
S	nozzle to late distance
UTS	ultimate tensile stress
PE	percentage elongation

Ferritic stainless steels, known for their superior corrosion resistance and affordability compared to austenitic stainless steels, are gaining popularity. These steels find widespread use due to their strong resistance to corrosion and ease of manufacturing. Low-chromium grades, in particular, are commonly employed in automotive exhaust systems.

To join ferritic stainless steels, austenitic stainless steels, Ni alloys, or filler metals with appropriate compositions can be used via fusion welding techniques. However, to prevent sensitization in the fusion zone, a very low carbon content is necessary. Additionally, the impact of filler metal dilution on weld structure and corrosion resistance must be carefully considered.

Ferritic stainless steel is a key material in metal inert gas (MIG) welding, a widely used process. Another unique arc welding method, gas metal arc welding (GMAW), is employed to join various commercial metals, including carbon steel, low- and high-alloy steel, stainless steel, copper, aluminum, titanium, zirconium, and nickel alloys. When combined with inert gas or gas mixtures, GMAW enhances weld quality. The process utilizes a consumable electrode, and its effectiveness depends on factors such as weld quality requirements, material properties, geometrical characteristics, and chemical aspects. Input parameters like gas flow rate, electrode output, current, voltage, welding position, edge preparation, and more significantly impact the overall weld quality.

Ferritic stainless-steel welding has been the subject of several studies [1–7], which are described below. Taban and associates. [1] investigated the mechanical, microstructural, and strength characteristics of various welds between carbon steel and ferritic stainless steel with 12% Cr modification. The effects of heat input on martensite formation and the characteristics of various ferritic-austenitic weld metals were investigated by Ferritic stainless-steel welding has been the subject of several studies [1–7], which are described below. Taban and associates. [1] investigated the mechanical, microstructural, and strength characteristics of various welds between carbon steel and ferritic stainless steel with 12% Cr modification. The effects of heat input on martensite formation and the characteristics of various ferritic-austenitic weld metals were investigated by Mukherjee and Pal [2]. Taban and associates. [3] also investigated the characteristics of ferritic stainless steel modified with 12% Cr when welded using three distinct consumables; in the end, they suggested using 309 and 316 welding wire for strong corrosion resistance. compared to 308 solder wire. Kah and associates. [4] Research on the weldability of ferritic stainless steels and their analysis demonstrated that the stabilization method can be used to provide adequate resistance to hot cracking during welding, as well as mechanical properties that are useful and resistance to intergranular cracking in the welded state. Shanmugam along with others. [5] The current study examines the effects of filler metals on the tensile and impact properties of ferritic stainless steel that complies with AISI grade 409M, including austenitic, ferritic, and duplex stainless steel. It was discovered that the tensile strength and hardness of joints constructed with duplex

Published by :
http://www.ijert.org

International Journal of Engineering Research & Technology (IJERT)
ISSN: 2278-0181
Volume 13, Issue 02, February 2024

stainless-steel filler metal are higher than those made with austenitic and ferritic stainless-steel filler metal. austenitic stainless-steel joints.

The impact of welding process variables on the mechanical and metallurgical properties of ferritic stainless-steel welds has not been extensively studied, according to a review of the literature. To improve the weld quality on the weld sample, it is crucial to select the ideal combination of parameters for MIG welding operations [8]. When it comes to designing, analysing, and optimizing process parameters for MIG welding operations, the Taguchi method of experimental design has proven to be effective [9]. In this work, the effects of gas flow rate, electric current, and nozzle-plate distance on the quality of the weld produced during MIG welding of ferritic stainless steel AISI 409 were investigated experimentally and analysed using the Taguchi method. Finally, complete content and organizational editing before formatting. Please take note of the following items when proofreading spelling and grammar

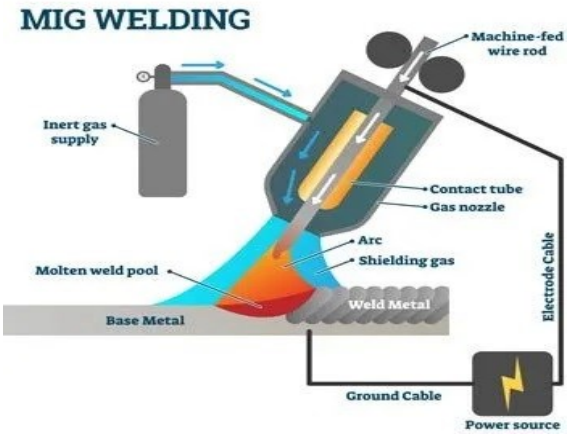

II. TAGUCHI METHOD

A quality management consultant from Japan named Dr. Genichi Taguchi created the Taguchi method. Designing for performance, quality, and cost can be done effectively and methodically with Taguchi's quality engineering methods, which make use of experimental designs. It is a crucial instrument for creating affordable, high-caliber systems. Process control parameters are optimally adjusted through the Taguchi method, which is based on orthogonal array experiments that significantly reduce experimental variance [10]. A balanced set of tests with fewer test runs is offered by orthogonal arrays. The signal-to-noise ratio, a statistical performance metric that accounts for both mean and variability, is used by the Taguchi method to assess the ideal parameterization. Quadratic quality loss function theory is explored by the Taguchi method. The ratio of the mean (signal) to the standard deviation (noise) is known as the signal-to-noise ratio, or S/N ratio. The product/process being optimized's quality attributes determine this ratio. NB, LB, and HB are the standard S/N ratios that are most frequently used. The parameter combination that yields the highest S/N ratio is the ideal configuration.

Taguchi's S/N Ratio (η) for nominal-the-best (NB):

$$\eta = 10\ ln_{10}\ \frac{1}{n}\sum_{i=1}^{n}\frac{\mu^2}{\sigma^2} \qquad (1)$$

Taguchi's S/N Ratio (η) for lower-the-better (LB):

$$\eta = -10\ ln_{10}\ \frac{1}{n}\sum_{i=1}^{n} y_i^2 \qquad (2)$$

Taguchi's S/N Ratio(η) for higher-the-better (HB):

$$\eta = -10\ ln_{10}\ \frac{1}{n}\sum_{i=1}^{n}\frac{1}{y_i^2} \qquad (3)$$

To ascertain the significance of each component in the output response, the Taguchi method employs signal-to-noise ratio analysis; the higher the ratio, the better the performance. The highest SNR value thus yields ideal parameter conditions.

III. EXPERIMENTAL PLAN, SETUP AND PROCEDURE

The experiments in this work were carried out in the order that was intended. The experimental design was based on the Taguchi L9 orthogonal array design. Three levels are taken into consideration for each of the input parameters: welding current, gas flow rate, and nozzle-to-plate distance. Table 1 displays the parameters and levels of the welding process. Table 2 displays the welding design matrix based on the L9 Taguchi orthogonal array design. Figure 1 depicts a welding installation process image.

Fig. 1 Photographic view of welding set-up

Table1. Welding process parameters and their levels

Factors	Unit	Notation	Levels		
			1	2	3
Welding Current	A	C	100	112	124
Gas Flow rate	*l*/min	G	10	15	20
Nozzle to Plate Distance	mm	S	9	12	15

Published by :
http://www.ijert.org

International Journal of Engineering Research & Technology (IJERT)
ISSN: 2278-0181
Volume 13, Issue 02, February 2024

Table 2. L9 orthogonal array of Taguchi method

Sample No.	Current (A)	Gas flow rate (*l*/min)	Nozzle to plate distance (mm)
1	100	10	9
2	100	15	12
3	100	20	15
4	112	10	12
5	112	15	15
6	112	20	9
7	124	10	15
8	124	15	9
9	124	20	12

Butt joints between 100 x 65 x 3 mm pieces of AISI 409 ferritic stainless steel are joined by MIG welding with AISI 316 L austenitic welding wire. Since austenitic stainless steel shouldn't be welded to be 3 mm thick, there is no need for edge preparation. One and a half millimeters was selected as the electrode wire's diameter. The ESAB AUTO K -400 MIG/MAG welding machine is used for welding. All of the weld samples underwent visual inspection and X-ray photographic examination because the butt welds were manufactured using various input parameters. Following X-ray and visual inspection, tensile samples were machined or cut from the welds. Small cut parts are also produced when tensile samples are cut or machined. To examine the microstructures, these tiny cut pieces are subsequently polished, ground, and etched. Section 3 reports the findings of the radiographic and visual inspection. Tensile specimens were put through ASTM-recommended testing on the INSTRON tensile testing apparatus. The following list contains the INSTRON tensile testing machine's primary technical specifications.

Model No. : 5589
Serial No. : 95/1058
Maximum capacity : 600 KN

A diagram showing the basic dimensions of a 3 mm thick tensile test specimen is given in Figure 2.

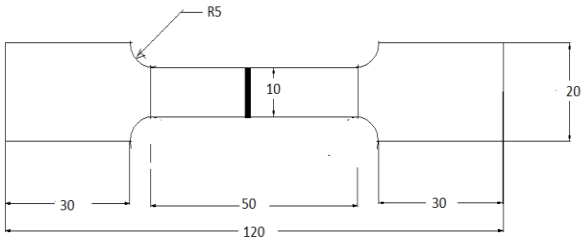

Fig. 2. Schematic diagram of the specimen prepared for tensile test

IV. RESULTS OF VISUAL INSPECTION AND X-RAY RADIOGRAPHIC TEST AND DISCUSSION

Following testing, the ferritic stainless-steel welded sample was subjected to visual inspection and X-ray photographic examination in order to identify any surface or subsurface defects. Since visual inspection serves as the primary foundation for the acceptance of many different types of welds, it is extremely important. Due to its ease of use, speed, affordability, and ability to yield crucial information regarding the weld and overall compliance of the welded structure with the requirements, this inspection method is the most popular one. method. Table 3 displays the findings from the radiographic and visual inspections. Figures 3 and 4 display some typical copies of X-ray films, respectively.

Fig. 3. Copies of X-ray radiographic film for sample no-4

Fig. 4. Copies of X-ray radiographic film for sample no-5

Table 3. Results of visual inspection and X-ray radiographic inspection

Sample no.	Result of visual inspection	Result of x-ray radiographic tests
1	no defects	no defects
2	blow hole, spatter	porosity
3	excessive deposition, spatter	lack of fusion
4	uneven penetration undercut	lack of fusion
5	spatter, uneven penetration	porosity
6	no defect	no defects
7	no defect	no defect
8	uneven penetration	lack of fusion
9	no defect	no defect

The defects discovered during the visual and radiographic inspection of welding samples obtained under various welding process parameter conditions—current, gas flow rate, and interval distance between nozzle and plate—are displayed in Table 3. Table 3 presents the findings from the visual inspection, which indicate that no defects were found under specific welding conditions. Those are sample numbers. 6, 7, and 9. Defects of the following kinds were discovered in some of the samples: undercuts and perforations, minor imperfections, and uneven penetration. Additionally, according to the X-ray test results (Table 3), samples No. have good comparison ratios. 6, 7, and 9. Defects like porosity and a lack of coherence can be present in some samples.

International Journal of Engineering Research & Technology (IJERT)
ISSN: 2278-0181
Volume 13, Issue 02, February 2024

When comparing the findings of the X-ray and visual inspections, some findings about sample flaws were consistent. In the course of the X-ray analysis, sample nos. 1, 6, 7, and 9 showed no discernible flaws. Upon visual inspection, these samples did not exhibit any defects. Once more for sample numbers. X-ray radiography tests for samples 2 and 5 as well as for some other samples (3, 4 and 8) revealed some notable defects like porosity and lack of adhesion. Additionally, some samples had flaws like cuts, perforations, excessive splash residue, and irregular penetration that were observed in the visual section. e. samples 2 through 5 and 8. The following is a discussion of potential causes of defects found during radiographic and visual inspection.

• Unevenness was discovered in some welded samples. The combined effect of gas flow level, current, and distance between nozzle and plate can increase or decrease the likelihood of potential causes of lack of penetration, undercutting, lack of melting, and deposition. In addition to gas flow rate, current, and nozzle-plate distance, other process-related variables (such as welding speed, welder proficiency, etc.) can also result in a combination of other defects. Once more, flaws may arise from the joints' mechanical architecture. Defects may also be related to metallurgy.

• Gases trapped in the solidified metal may be the cause of porosity and blow holes. Greater arc size, increased travel speed, excessively high or low arc current, improper welding technique (wire ball or woven bead, etc.), a dirty work surface, and a wet welding rod are the usual causes of porosity and blow holes.

• Inadequate joint geometry for some samples and an unfavorable combination of current, gas flow, and distance from the nozzle to plate could be the cause of the undercuts discovered under some conditions in the current study. The undercut phenomenon may also be caused by larger arcs or faster arc travel speeds during welding.

• Insufficient current, a faster-moving arc, or a technique that is not appropriate for the welding process could be the cause of the lack of fusion seen in some specimens welded under specific current, gas flow, and nozzle-to-plate distance conditions. improper handling of the electrode or feed bar, improper preparation, improper seal adjustment, oxides, deposits, and other impurities (on the weld surface) that prevent the deposited metal from properly combining with the base metal, etc.

• Inadequate current settings, the relationship between gas flow and plate distance, poorly held electrodes, faster arc travel speeds, and too-small pin gaps can all contribute to a lack of penetration. Based on a visual examination, there might be too much filler metal on the plate. posterior aspect of the joint, and the original segment is typically connected to it.

• Spatters, which are exclusive to sample nos. 2, 3, and 5 could be the result of electric arcs, wet filler rods, or gas bubbles trapped in the molten metal drop that explode intensely and shoot tiny metal drops out of the arc suture.

• Higher gas flow can lead to improved resistance to air pollution, which enhances the quality of the weld. On the other hand, a large increase in gas flow may result in turbulence, which can guard against uncontrolled arc and weld puddles while raising the possibility of gas absorption from the surroundings. One can draw comparisons between the effect previously mentioned and the air flow effect reported in this study. An essential component of any arc welding process is current. Both high and low currents have benefits and drawbacks. Appropriate current configurations offer the required blend, penetration, and power output. The metallurgical quality of the weld and the heat-affected zone are ultimately determined by the energy input, the rate of energy input, and the heating and cooling cycles involved in any arc welding process. The distance between the nozzle and the plate, another welding parameter, also has an impact on the welded sample's quality.

V. TENSILE TEST RESULTS AND DISCUSSION

The experiment outcomes are shown in Table 4. Utilizing statistical methods like main effects plots and signal-to-noise ratio analysis, the significance of the weld parameters in relation to the output response (i.e. e. the ultimate elongation rate and tensile strength). of the sample welded. Using the Taguchi method, the response parameters (elongation ratio and ultimate tensile strength) were optimized to determine the best possible parameter combination that would result in the desired quality of welds. desire by examining two different answers.

Table 4. Output results

Sample No.	Output responses	
	Ultimate tensile strength (mpa)	Percentage of elongation (%)
1	431.6	25.5
2	376.5	15.05
3	377.3	18.53
4	416.6	17.6
5	368.3	24.5
6	424.0	17.0
7	431.6	25.5
8	423.5	18.0
9	453.6	23.4

5.1. Analysis of signal-to-noise ratio for ultimate tensile strength (UTS) and percentage of elongation (PE)

The MINITAB 16.1 software uses a statistical technique called signal-to-noise ratio analysis to analyze experimental data and identify the welding parameters that significantly impact quality characteristics. These parameters include the weld's ultimate tensile stress (UTS) and percent elongation (PE). ferrites. stainless steel substance. Tables 5 and 6 show the signal-to-noise ratio analysis for PE and UTS, respectively. At a significance level of five percent, or the 95 percent confidence interval, the analysis of variance was conducted. Should the noteworthy amount, i.e. e. At the 95 percent confidence level, the corresponding value in the ANOVA table is deemed significant if the P value is greater

International Journal of Engineering Research & Technology (IJERT)
ISSN: 2278-0181
Volume 13, Issue 02, February 2024

than 0.05. The ANOVA results of the two responses (Tables 5 and 6) show that the process parameters have a significant influence on UTS because their P value is close to 0.05 compared to PE. Based on the ANOVA tables of UTS (Table 5) and PE (Table 6), it appears that all welding process parameters do not have a significant influence on both reactions.

Table 5. Analysis of signal-to-noise ratio for ultimate tensile strength (UTS)

Source	DF	Seq SS	Adj MS	F	P
C	2	1.28606	0.64303	15.92	0.059
F	2	1.06457	0.53228	13.18	0.071
S	2	0.85680	0.42840	10.61	0.086
Residual Error	2	0.08077	0.04038		
Total	8	3.28819	R-Sq = 97.5%		

Table 6. Analysis of signal-to-noise ratio for percentage of elongation (PE)

Source	DF	Seq SS	Adj MS	F	P
C	2	10.8087	5.4043	5.95	0.144
F	2	15.0706	7.5353	8.29	0.108
S	2	0.6857	0.3428	0.38	0.726
Residual Error	2	1.8176	0.9088		
Total	8	28.3825	R-Sq = 93.6%		

5.2. Factor effects

Using MINITAB 16.1 software, the main effects plots for UTS and PE were created from experimental data, and they are displayed in Figs. Five and Six. The direct impact of this factor on the response variable can be examined using the main effect plots. The impact on variable responses increases with the difference between the lower and higher levels within each level in the main effects plot. According to the UTS main effect diagram, the welding current parameter (C), gas flow rate (G), and distance between the nozzle and plate (S) have the greatest effects. Diagram illustrating EP's primary effects (Figure 2). 6) demonstrates that welding current (C) is the second most important factor for PE, after gas flow rate (G). As seen in Fig., the welding coefficient and nozzle-to-plate distance (S) have less of an impact on PE. 6. The plot of UTS and PE main effects at the maximum signal-to-noise ratio value also provides the ideal parameter conditions to maximize the output response. The ideal parameter values were determined to be current (C) = 124 A, gas flow rate (G) = 10 l/min, and distance (S) = 9 mm from the spray nozzle to the plate (based on the main effects plots of UTS and PE)

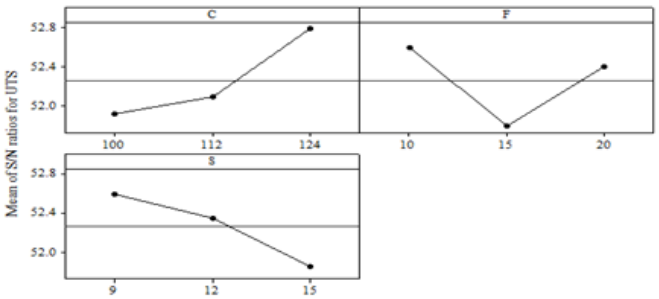

Fig. 5. Main effect plots for ultimate tensile stress (UTS)

VI. CONFIRMATORY EXPERIMENT

To confirm that the best outcomes from the Taguchi method were indeed optimal, confirmation experiments were run with optimal parameter configurations. In comparison to the first experiments (Table 4), the validation results shown in Table 6 validate the maximum responses with ideal parameter settings.

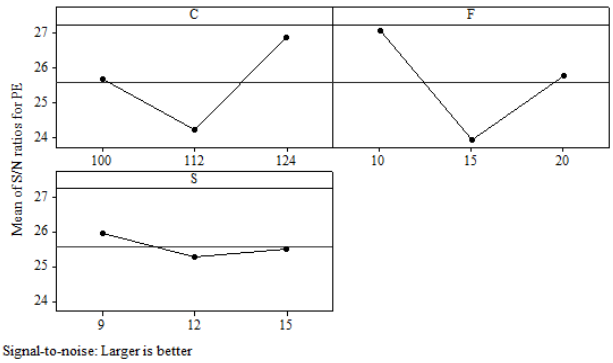

Fig. 6. Main effect plots for and percentage elongation (PE)

VII. CONCLUSIONS

The following important are drawn from the present study of MIG welding of ferritic stainless steel materials:

•Results of visual inspection indicate that undercut and blow holes have been found in few samples, uneven deposition, and excessive penetration have also been found in some samples.

•Results of X-ray radiography test indicate: lack of penetration, low – level porosity, lack of fusion, weld depressions and surface mark in some of the samples.

•Results of visual inspection and X-ray radiographic tests are compared, some consistency are founds.

•ANOVA test results indicate that welding process parameters do not have significant influence on both the responses.

•Optimal parametric welding condition is (i.e. current (C) = 124 A, gas flow rate (G) = 10 l/min and nozzle to late distance (S) = 9 mm) obtained by Taguchi method for maximizing both the responses: UTS and PE

•Confirmatory experiment results confirm the validity of the optimal results obtained by Taguchi method.

•Taguchi experimental design method is very useful to analyze the welding of ferritic stainless steels in MIG welding operation

International Journal of Engineering Research & Technology (IJERT)
ISSN: 2278-0181
Volume 13, Issue 02, February 2024

VIII. REFERENCES

[1] E.Taban et al., Evaluation of Dissimilar Welds between Ferritic Stainless Steel Modified 12% Cr and Carbon Steel S355, American Welding Society and the Welding Research Journal, (2012) 291-297.
[2] M. Mukherjee, T.K. Pal, Influence of Heat Input on Martensite Formation and Impact Property of Ferritic-Austenitic Dissimilar Weld Metals, J. Mater. Sci. Technol, 28(4) (2012) 343-352.
[3] Metals Handbook, vol. 6, 9th edition, p. 320-352.
[4] D. H. Kah, D. W. Dickinson, Weldability of Ferritic Stainless Steels, American Welding Society and the Welding Research Journal, (1981) 135-141.
[5] K. Shanmugam, A.K. Lakshminarayanan, V. Balasubramanian, Tensile and Impact Properties of Shielded Metal Arc Welded AISI 409M Ferritic Stainless Steel Joints, J. Mater. Sci. Technol, 25 (2009) 181.
[6] ASM Handbook, Vol. 8, Mechanical Testing, 9th edition, p 30-466.
[7] P. Sonasale, An Approach to Optimize MIG Welding Parameters by Using Design of Experiments, Adv. Materials Manufacturing & Characterization, 5 (2015) 24-34.
[8] N. Murugan, R.S. Parmer, Effect of MIG Process Parameters on the Geometry of the Bead in the Automatic Surfacing of Stainless Steel, J. Mater. Process. Technol. 41 (1994) 381–398.
[9] I.S. Kim, C.E. Park, K.D.V. Prasad, Yarlagadda, A study on the Prediction of Process Parameters in the Gas-Metal Arc Welding (GMAW) of Mild Steel using Taguchi Methods, Mater. Sci. Forum, (2003) 235– 238.
[10] R.K. Kesharwani, S.K. Panda, S.K. Pal, Multi Objective Optimization of Friction Stir Welding Parameters for Joining of Two Dissimilar Thin Aluminum Sheets, Procedia Material Science, 6 (2014) 178-187.